Effect of Surface Heave on Response of Partially Embedded Pipelines on Clay

R. S. Merifield[1]; D. J. White[2]; and M. F. Randolph[3]

Abstract: The as-laid embedment of an on-bottom pipeline strongly influences the resulting thermal insulation, and the resistance to subsequent axial and lateral movement of the pipeline. Reliable assessment of these parameters is essential for the design of offshore pipelines. Static vertical penetration of a pipe into a soft clay seabed—which can be modeled as an undrained process—causes heave of soil on each side of the pipeline. The heaved soil contributes to the vertical penetration resistance and the horizontal capacity. This paper describes a series of large deformation finite-element analyses of pipe penetration, supported by a simple analytical assessment of the heave process. The conventional bearing capacity approach to the analysis of pipe penetration is reviewed, and modifications for the effects of soil weight and heave are presented. It is shown that in soft soil conditions—which are typical for deep water—the soil self-weight contributes a significant portion of the vertical penetration resistance and horizontal capacity. If heave is neglected, the soil weight leads to a vertical force due to buoyancy, based on Archimedes' principle. When heave is considered, the soil weight contributes an additional component of vertical load, exceeding simple buoyancy, due to the distorted geometry of the soil surface. Archimedes' principle does not apply. The finite-element analyses, benchmarked against rigorous plasticity solutions, are used to calibrate simple expressions for predicting static vertical pipe penetration, and the resulting horizontal capacity. These simple solutions allow the conventional bearing capacity approach to be used in a manner which correctly accounts for the effects of soil self-weight and heave. An approximate solution for predicting the "local" pipe embedment—relative to the raised soil level immediately adjacent to the pipe—is derived. The local embedment significantly exceeds the nominal embedment relative to the original soil surface. This effect counteracts the tendency for heave to reduce the embedment by raising the penetration resistance.

DOI: 10.1061/(ASCE)GT.1943-5606.0000070

CE Database subject headings: Pipelines; Clays; Plasticity; Offshore structures; Finite element method; Soil mechanics; Collapse loads; Cohesive soils; Embedment.

Introduction

Background

As the development of oil and gas resources extends into deeper water, the associated pipelines represent an increasing fraction of the capital expenditure. In deep water, pipelines are usually laid directly on the seabed, rather than being trenched and buried, since there is no need for protection from overtrawling and they are designed to buckle during thermal expansion. During the laying process, the pipe typically penetrates into the seabed by a fraction of a diameter.

Pipelines usually operate at high temperature and pressure, resulting in significant loading when they are heated compared with the as-laid condition. The axial stress induced by the change in temperature and pressure causes a tendency for the pipeline to buckle in operation, and break out from the initial partially embedded position. This buckling must be prevented or controlled. The buckling response depends on the initial breakout resistance, which is in turn strongly influenced by the pipe embedment. Controlled lateral buckling can represent a cost-effective solution to the problem of thermal loading, but requires reliable assessment of the pipe-soil resistance (Bruton et al. 2008). Robust methods for assessing the embedment and breakout resistance of partially embedded pipelines are therefore essential for the design of deepwater pipelines.

Objectives

Current calculation methods for assessing the penetration of a pipeline into soft clay—which is the most common deep water seabed sediment—are often empirically based on model test data (DNV 2007). Theoretical solutions from classical plasticity analysis, in which the soil is modeled as a rigid-plastic Tresca material with shear strength s_u, offer a more robust basis for linking vertical load, V, to pipe embedment, w [Fig. 1(a)]. Murff et al. (1989) and Aubeny et al. (2005) present plasticity solutions for the vertical penetration of a "wished-in-place" shallowly embedded pipe, providing a theoretical link between normalized vertical load, V/s_uD, and normalized pipe penetration, w/D. Merifield et al. (2008) and Randolph and White (2008) present improved solu-

[1]Senior Lecturer, Centre for Geotechnical and Materials Modelling, Univ. of Newcastle, University Dr., Callaghan, Newcastle 2308, NSW, Australia (corresponding author). E-mail: richard.merifield@newcastle.edu.au

[2]Professorial Fellow, Centre for Offshore Foundation Systems, Univ. of Western Australia, Stirling Highway, Crawley 6009, WA, Australia. E-mail: white@civil.uwa.edu.au

[3]ARC Federation Fellow, Professor, Centre for Offshore Foundation Systems, Univ. of Western Australia. E-mail: randolph@civil.uwa.edu.au

Note. This manuscript was submitted on February 12, 2008; approved on September 29, 2008; published online on February 19, 2009. Discussion period open until November 1, 2009; separate discussions must be submitted for individual papers. This paper is part of the ***Journal of Geotechnical and Geoenvironmental Engineering***, Vol. 135, No. 6, June 1, 2009. ©ASCE, ISSN 1090-0241/2009/6-819–829/$25.00.

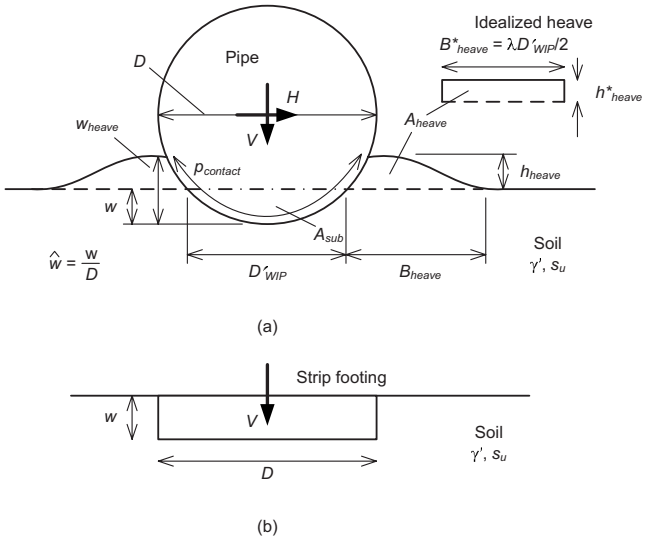

Fig. 1. Nomenclature

tions for the vertical response, and also consider combined vertical and horizontal loading, generating yield envelopes of allowable *V-H* load combinations.

These previous analyses were based on a "wished-in-place" (WIP) pipe embedded within horizontal ground—such that the pipe is in contact with the soil over the nominal effective diameter D'_{WIP} [Fig. 1(a)]. Nonlinear geometric (or "large deformation") effects were neglected. In reality, heave is generated as the soil is displaced by the pipe, increasing the contact width between the pipe and the soil as shown schematically in Fig. 1(a). This heaved soil increases the resistance to further vertical penetration and horizontal movement.

In their state-of-the-art review of pipeline geotechnics, Cathie et al. (2005) noted the importance of heave in raising the penetration resistance compared to WIP calculations, and highlighted the scope for further theoretical work in this area. The purpose of this paper is to tackle this issue by presenting analyses in which the pipe is "pushed-in-place" (PIP). These analyses quantify the effect of surface heave on the resistance to vertical penetration and lateral breakout, allowing more realistic calculations to be proposed for design. First, the existing bearing capacity methods that apply to the WIP case are described, and the methodology for extending these solutions to the PIP case is set out.

Bearing Capacity Solutions

Bearing Capacity of Embedded Strip Footings

A strip footing embedded below a horizontal ground surface represents a simplification of the circular geometry of a partially embedded WIP pipe, and is the starting point for the modifications necessary to apply the bearing capacity approach to PIP pipes.

For undrained conditions, the vertical bearing capacity of an embedded strip footing of width D is assessed using Eq. (1*a*) and (1*b*) [Fig. 1(b)]. The nominal vertical bearing stress—expressed as $q=V/D$, where V, the vertical load relative to the submerged weight of the footing, is composed of two superimposed contributions, which are linked to the effects of soil strength and self-weight (which leads to buoyancy)

$$\frac{V}{D} = q = N_{cV} s_u + N_{swV} \gamma' w \quad \text{(general)} \tag{1a}$$

Two factors are defined to link the strength, s_u, and weight $\gamma' w$, to the bearing stress; q=usual vertical bearing capacity factor, N_{cV}, and also a factor referred to in this paper as the "self-weight factor" N_{swV}. For a surface strip footing, the bearing capacity factor, N_{cV}, is equal to the Prandtl (1921) solution of $(2+\pi)=5.14$. If the footing is embedded to a depth w/D, then the failure mechanism includes shearing of the soil adjacent to the footing, and N_{cV} can be expressed as a function of w/D (Skempton 1951; Salgado et al. 2004; Gourvenec 2008). The self-weight factor $N_{swV}=1$, can be deduced from the change in potential energy of the soil during an increment of vertical footing penetration, δw, noting that the ground surface is initially level. The soil displaced at the footing base has a potential energy of $(\gamma' D \delta w) w$ relative to a datum of zero at the surface, $w=0$. The bracketed term is the weight of soil displaced by the footing. By continuity, the same volume of soil must heave at the ground surface, where the potential energy is zero. Therefore, by equating the component of the work done on the footing against the soil self-weight, to the gain in potential energy, it can be shown that $N_{swV}=1$.

This is simply a statement of Archimedes' principle of buoyancy. In the limit, as the soil strength tends to zero ($s_u/\gamma' w \rightarrow 0$), Eq. (1*a*) shows that the force on the footing, V, is equal to the weight of the displaced soil, $\gamma' wD$. Eq. (1*a*) can be recast with the self-weight term expressed in terms of Archimedes' principle, where $N_{swV}=f_b A_s/Dw$

$$\frac{V}{D} = q = N_{cV} s_u + (f_b \gamma' A_s)\frac{1}{D} \quad \text{(general)} \tag{1b}$$

The bracketed term gives the buoyancy force where A_s =submerged cross-sectional area of the foundation. If $f_b=1$ then this term is Archimedes' principle: the upwards buoyancy force equals the weight of the displaced fluid. As discussed later, the factor f_b exceeds unity if the embedment of the foundation creates heave, altering the geometry of the soil surface. The equivalent general expression for failure in the horizontal direction can be expressed as

$$\frac{H}{D} = N_{cH} s_u + N_{swH} \gamma' w \quad \text{(general)} \tag{2}$$

For a surface strip footing (with a rough base) displaced horizontally the failure mechanism simply involves sliding at the base of the footing, where a shear stress of s_u is mobilized. Therefore, $N_{cH}=1$ and the self-weight term is zero, since $w=0$. N_{cH} rises linearly with embedment, due to the passive resistance of the soil adjacent to the foundation (Gourvenec 2008; Bransby and Randolph 1999). If the soil behind the foundation is assumed to collapse into any void created when the footing moves horizontally, then the net potential energy of the soil domain is unchanged, so $N_{swH}=0$.

However, if a crack opens behind the foundation and this soil stands vertically, then the soil domain will undergo a net gain in potential energy, due to the heave ahead of the footing. During a small horizontal movement of δu, the potential energy gain of the soil domain is $(\gamma' w \delta u)\bar{z}$ where the bracketed term is the weight of soil displaced by the footing and $\bar{z}$ is the mean elevation of the displaced soil relative to the ground surface—which is equal to $w/2$. From Eq. (2), the component of the work done by H against

the soil weight is $N_{swH}\gamma' wD\delta u$. Therefore, for an embedded strip footing with a stable open crack at the rear (expressing the normalized embedment, w/D as $\hat{w}$)

$$N_{swH} = \frac{\hat{w}}{2} \quad \text{(embedded strip)} \tag{3}$$

The same result can be obtained by performing a simple Coulomb wedge analysis. To highlight the relative contributions of the strength and self-weight terms, Eq. (1*a*) and (1*b*) can be rewritten as

$$\frac{V}{Ds_u} = N_{cV} + N_{swV}\frac{\gamma' w}{s_u} \quad \text{(general)} \tag{4}$$

The contribution of the self-weight term can be significant in soft soils (i.e., high $\gamma' w/s_u$). Very soft seabed clays generally show a small strength intercept at the mudline (typically ~0.5 kPa) together with a strength gradient (typically ~1 kPa/m). For shallow seabed structures, such as on-bottom pipelines, based on an embedment depth of 0.5 m and $\gamma' = 6$ kN/m^3, these values indicate a practical upper limit of $\gamma' w/s_u = 3$.

For the case of a strip footing at an embedment of $\hat{w} = 0.25$, for which $N_{swV} = 1$ and $N_{cV} \sim 6.2$ (Salgado et al. 2004; Gourvenec 2008), Eq. (4) shows that the soil self-weight contributes up to ~30% of the total vertical bearing capacity, which represents a significant fraction of the overall resistance. The following analysis investigates the corresponding effect in the case of a partially embedded pipe, for which the curved pipe geometry alters the values of N_{cV} and N_{swV}.

Bearing Capacity Solutions for WIP Pipes

The bearing stress, q, in Eq. (1*a*) and (1*b*) is defined based on the full pipe diameter, D, as $q = V/D$. Values of N_{cV} have been presented for WIP pipes by Murff et al. (1989), Aubeny et al. (2005), and Merifield et al. (2008), based on failure mechanisms assessed by plasticity limit analysis and finite-element analysis. Analyses presented by Merifield et al. (2008) for the range $0 \leq \hat{w} \leq 0.5$, gave the following fit, assuming that tension could not be sustained at the pipe-soil interface:

$$N_{cV} = 5.66(\hat{w})^{0.32} \quad \text{(smooth WIP pipe)} \tag{5}$$

For a rough pipe, the corresponding fitted expression was

$$N_{cV} = 7.4(\hat{w})^{0.4} \quad \text{(rough WIP pipe)} \tag{6}$$

These analyses neglected the effect of soil self-weight. For the WIP case, with a horizontal ground surface, the self-weight factor N_{swV} can be assessed analytically by considering the potential energy of the displaced soil around the periphery of the pipe—that is, Archimedes' principle. The curved pipe geometry leads to a more complicated expression than derived previously for an embedded strip footing, given by

$$N_{swV} = \frac{1}{4\hat{w}}\left[\sin^{-1}\left(\sqrt{4\hat{w}(1-\hat{w})}\right) - 2(1-2\hat{w})\sqrt{\hat{w}(1-\hat{w})}\right] \quad \text{(WIP pipe)} \tag{7}$$

For the same embedment as considered for an embedded strip footing ($\hat{w} = 0.25$), the bearing capacity factors for a smooth pipe are $N_{cV} = 3.63$ and $N_{swV} = 0.61$. The self-weight contribution is therefore 50% of the penetration resistance, for $\gamma' w/s_u = 3$, representing a slightly larger contribution than for a strip footing embedded at the same depth.

For the case of horizontal failure [Eq. (2)], the results presented Merifield et al. (2008) led to the following expression for the horizontal bearing capacity factor, N_{cH}:

$$N_{cH} = 2.72(\hat{w})^{0.78} \quad \text{(smooth WIP pipe)} \tag{8}$$

For a rough pipe, the corresponding fitted expression was

$$N_{cH} = 3.26(\hat{w})^{0.82} \quad \text{(rough WIP pipe)} \tag{9}$$

The self-weight factor for horizontal failure (in which the soil behind the pipe is assumed to remain standing) is the same as for an embedded strip footing, since the mean elevation of the displaced soil is the same, therefore

$$N_{swH} = \frac{\hat{w}}{2} \quad \text{(WIP pipe)} \tag{10}$$

Bearing Capacity Solutions for PIP Pipes

For the PIP case, the heaved soil is sheared during vertical or horizontal pipe movement, creating additional resistance compared to the WIP case. This results in slightly higher values of N_{cV} and N_{cH}. Also, the self-weight term is modified for a PIP pipe because the surface heave during an increment of penetration is added to the top of the pre-existing heave profile, leading to a greater change in the potential energy of the soil. As a result, the self-weight term is greater than that calculated using a not simple buoyancy expression.

To generate an analytical approximation for the self-weight component of the bearing capacity, the previously heaved soil can be idealized as a rectangular block [Fig. 1(a)] upon which the next increment of heave is added. The width of the idealized heave block, B^*_{heave}, is assumed to increase in proportion to the nominal contact width of the pipe [so $B^*_{\text{heave}} = \lambda D'_{\text{WIP}}/2$, where the berm geometry parameter λ is defined in Fig. 1(a)], reflecting the increasing lateral extent of the failure mechanism as the pipe penetrates deeper.

The height of the idealized heave block, h^*_{heave}, is assumed to equal the mean elevation of the next increment of soil heave. This is a crude idealization, which neglects the requirement that some heave must occur at the ground surface in order for the width of the heaved zone to increase. However, by defining an elevation at which the next increment of heave is lumped, the analytical self-weight factors, N_{swV} and N_{swH} derived previously for the WIP case can be extended to the PIP case.

From continuity, the dimensions of the idealized heave profile can be calculated as

$$\frac{B^*_{\text{heave}}}{D} = \lambda\sqrt{\hat{w}(1-\hat{w})} \quad \text{(PIP pipe)} \tag{11}$$

$$\frac{h^*_{\text{heave}}}{D} = \left(\frac{1}{4\lambda}\right)\left[\frac{\sin^{-1}\left(\sqrt{4\hat{w}(1-\hat{w})}\right)}{2\sqrt{\hat{w}(1-\hat{w})}} - (1-2\hat{w})\right] \quad \text{(PIP pipe)} \tag{12a}$$

A simplification of this expression, which is accurate to within 10% for practical values of λ, is

$$\frac{h^*_{\text{heave}}}{D} \approx \frac{\hat{w}}{1.4\lambda} \quad \text{(PIP pipe)} \tag{12b}$$

This simplification defines the berm shape in terms of h^*_{heave} which is a multiple of the embedment, rather than B^*_{heave} which is a multiple of the contact width. Eq. (12*a*) defines the elevation at

which heave occurs, from which an analytical approximation to the vertical self-weight term, N_{swV}, can be derived

$$N_{swV} = \frac{1}{2\hat{w}}\left(1 + \frac{1}{\lambda}\right) \times \left[\frac{\sin^{-1}(\sqrt{4\hat{w}(1-\hat{w})})}{2} - (1-2\hat{w})\sqrt{\hat{w}(1-\hat{w})}\right] \quad \text{(PIP pipe)} \tag{13}$$

The expression can be recast so that the self-weight term in Eq. (1*a*) and (1*b*) can be expressed in terms of a multiplier, f_b, which is in turn related to the simple fluid buoyancy defined by Archimedes' principle. The nominal submerged area of the pipe is

$$A_s = \frac{D^2}{4}[\sin^{-1}(\sqrt{4\hat{w}(1-\hat{w})}) - 2(1-2\hat{w})\sqrt{\hat{w}(1-\hat{w})}] \tag{14}$$

Therefore, the buoyancy multiplier, f_b, [in Eq. (1*b*)] is related to the berm geometry parameter, λ, by

$$f_b = (1 + 1/\lambda) \tag{15}$$

For the case of horizontal movement (assuming that the soil behind the pipe remains standing), the corresponding self-weight factor, N_{swH}, is

$$N_{swH} = \frac{\hat{w}}{2} + \left(\frac{1}{4\lambda}\right)\left[\frac{\sin^{-1}(\sqrt{4\hat{w}(1-\hat{w})})}{2\sqrt{\hat{w}(1-\hat{w})}} - (1-2\hat{w})\right] \quad \text{(PIP pipe)} \tag{16}$$

Large deformation numerical analyses using the finite-element method have been conducted to calibrate the berm geometry parameter λ—and to calculate the variation in N_{cV} and N_{cH} for PIP pipes.

Potential Effect of Self-Weight on Failure Mechanism for PIP Pipes

The numerical investigation described later considered soils with a normalized weight of $\gamma' D/s_u = 0$ (weightless), 1, 3, and 6, where the last represents a practical upper limit. This parametric study was necessary because the effects of self-weight and soil strength are not necessarily independent for the PIP case. The self-weight of the soil may influence the failure mechanism—and therefore the bearing capacity factor—for a PIP pipe. The source of this interaction is as follows. For the WIP case, the volume of soil displaced by the pipe during a small increment of penetration causes an equal volume of heave at the ground surface. The net change in the potential energy of the soil cannot be altered by a change of the failure mechanism, since all points on the ground surface have the same potential energy.

However, for a PIP pipe, the surface heave during an increment of penetration is added to the top of the existing heave profile. Therefore, the mean change in elevation of the displaced soil depends on the distribution of the incremental heave along the pre-existing heaved surface. The work done against the soil self-weight is reduced by a wider heave profile—extending toward the undisturbed ground surface remote from the pipe. However, a wider heave profile increases the size of the failure mechanism, increasing the work done against the soil strength.

In the limit, as $\gamma' w/s_u \to \infty$, the soil is simply a heavy fluid, so the ground surface remains flat. Archimedes' principle then applies, and the self-weight factor, N_{swV}, for the WIP case will also apply for a PIP pipe. For the heave idealization described previously, as $\gamma' w/s_u \to \infty$ then $\lambda \to \infty$. In contrast, for realistic values of $\gamma' w/s_u$, the heave will lead to additional soil potential energy, and a higher value of N_{swV} will apply in PIP conditions compared to the WIP case.

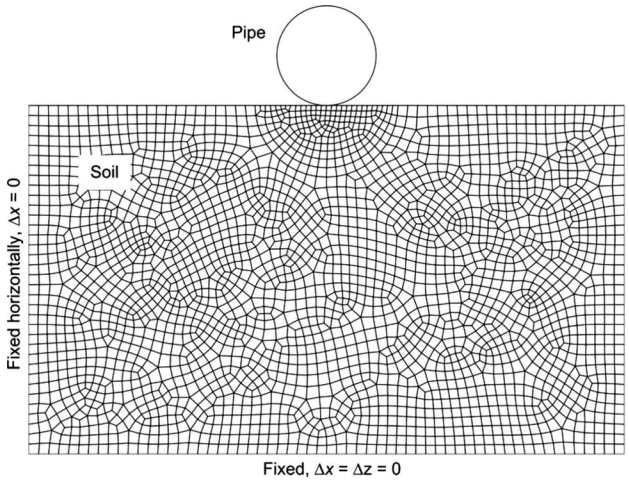

Fig. 2. Finite-element mesh and boundary conditions

Finite-Element Analysis: Methodology

Numerical Techniques

The finite-element analyses were conducted using ABAQUS software (HKS 2004). A total of 160 analyses were conducted, from which values of N_c and N_{sw} were back-calculated for vertical and horizontal failure. Plane strain conditions were imposed, and the model consisted of two parts: the pipe and the soil. A large deformation formulation was used, in conjunction with arbitrary Lagrangian–Eulerian (ALE) remeshing, allowing the pipe invert to be penetrated from the ground surface to the final embedment of $w/D = 0.5$, without incurring geometry-related errors. A typical mesh, along with the applied displacement boundary conditions, is shown in Fig. 2. The actual distribution and concentration of elements varied throughout the analyses, as controlled by the mesh adaptivity process within ABAQUS. The unstructured mesh was primarily comprised of four-noded quadrilateral plane strain elements which were found to provide the best solution convergence. The overall mesh dimensions were selected to ensure that the zones of plastic shearing and the observed displacement fields were contained within the model boundaries at all times. Further details of the numerical approach are given by Merifield et al. (2008).

The soil was modeled as a uniform isotropic elastic-perfectly plastic continuum with failure described by the Tresca yield criterion, characterized by the limiting shear stress, denoted s_u. The elastic behavior was defined by a Poisson's ratio $\nu = 0.49$, and a ratio of Young's modulus to shear strength of $E/s_u = 500$. Because the pipe is much stiffer than the soil it comes into contact with, and as the stresses in the pipe are of no concern in this case, the pipe was modeled as a discrete rigid body.

The collapse load was evaluated as the steady load reached when the pipe was displaced either vertically (to evaluate N_{cV} and N_{swV}) or horizontally (to evaluate N_{cH} and N_{swH}).

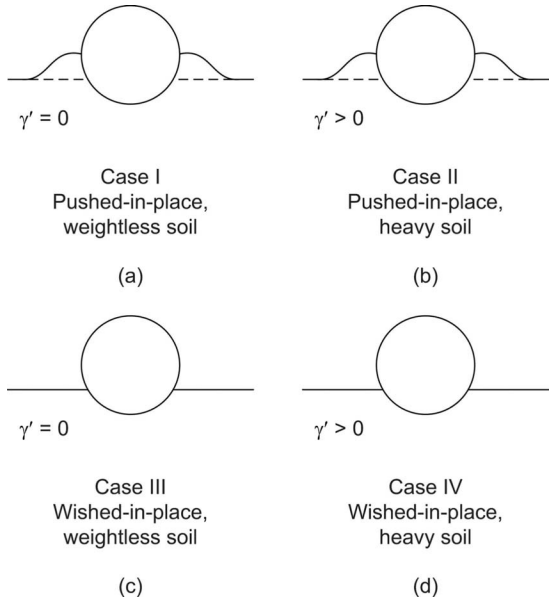

Fig. 3. Pipe-soil embedment cases

Sequence of Analyses and Interpretation

Eight different parameter sets were analyzed for the PIP case: rough and smooth pipe-soil interface, together with normalized soil weights of $\gamma' D/s_u=0$ (weightless), 1, 3, and 6. For each parameter set, an initial analysis involving purely vertical penetration to an embedment of $w/D=0.5$ was conducted. (Fig. 3, Cases I and II).

The relevant intermediate and final steps of each analysis were used as the initial conditions for a horizontal displacement of the pipe, to allow the horizontal collapse load to be assessed at embedment intervals of $0.1D$. The limiting loads recorded for the weightless case were used to assess PIP values of N_{cV} and N_{cH} [based on Eqs. (1*a*), (1*b*), and (2), with $\gamma'=0$].

By assuming that the value of N_{cV} is unaffected by $\gamma' D/s_u$, the limiting loads from the three $\gamma' D/s_u>0$ cases were then used to calculate the self-weight factors, N_{swV} and N_{swH}. It was found that the limiting loads increased linearly with the soil weight, implying constant values of N_{swV} and N_{swH} if N_{cV} and N_{cH} are assumed to be unchanged. This could indicate that the strength and self-weight factors are indeed independent of $\gamma' D/s_u$ and may be superimposed. Alternatively, they could vary with $\gamma' D/s_u$ in opposite proportions, leading to no net effect on the capacity. In either case, this parametric study indicates that the strength and self-weight contributions to the vertical bearing capacity (and horizontal limit load) can be assessed independently over the range $0<\gamma' D/s_u<3$.

Similar analyses for the weightless WIP case (Fig. 3, Case III) have been presented previously by Merifield et al. (2008), and are reproduced here for comparison. Further analyses have been conducted with heavy soil and a WIP pipe (Fig. 3, Case IV), to confirm the analytical expressions for N_{swV} [Eq. (7)] and N_{swH} [Eq. (10)] for the WIP case.

Finite-Element Analysis: Results

Vertical Response: N_{cV} and N_{swV}

The results of the finite-element analyses are summarized by the bearing capacity factors shown in Figs. 4 (N_{cV}) and 6 (N_{cH}), and the self-weight factors shown in Figs. 5 (N_{swV}) and 7 (N_{swH}). Separate subfigures show the results for the smooth and rough interface cases. The WIP FE results presented by Merifield et al. (2008) are labeled "FE: WIP" throughout, and the PIP FE results from this study are labeled "FE: PIP." The results from the WIP upper bound plasticity solutions presented by Randolph and White (2008) are labeled "UB: WIP."

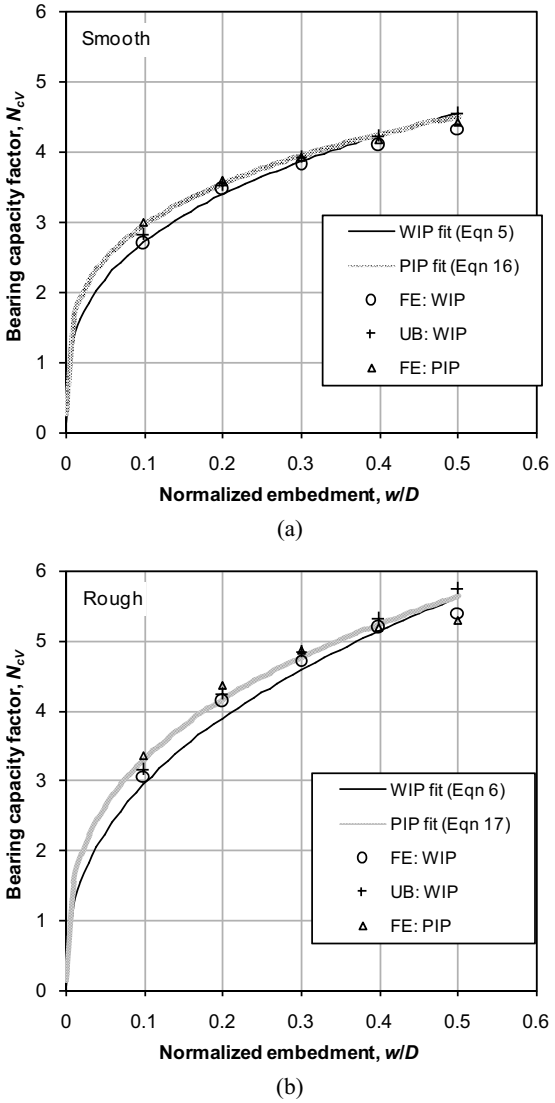

Fig. 4. Bearing capacity factors for vertical penetration

The shearing of the heaved soil in the PIP case leads to an increase in the bearing capacity factor, N_{cV} compared to the WIP case, for both rough and smooth interfaces (Fig. 4); the increase is most significant at shallow embedment. For initial embedment, the upper bound mechanism described by Murff et al. (1989) is optimal. This mechanism involves shearing within the soil close to original seabed level—and therefore also the heaved material for the PIP case. For greater embedment, the mechanism using rotating rigid blocks described by Martin and Randolph (2006) is applicable. Since these blocks grow in size with increasing embedment, the heave zone close to the pipe has less influence.

Adjustment of the fitted expressions given by Eqs. (5) and (6) for the WIP case leads to the following curve fits to the PIP results, which are also shown in Fig. 4:

$$N_{cV}=5.3(\hat{w})^{0.25} \quad \text{(smooth PIP pipe)} \tag{17}$$

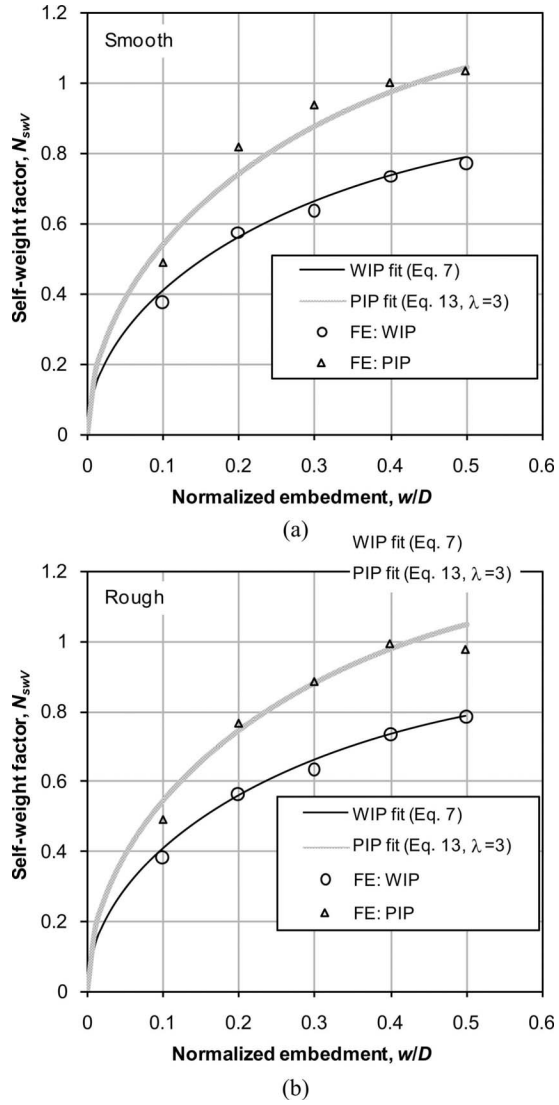

Fig. 5. Self-weight factors for vertical penetration

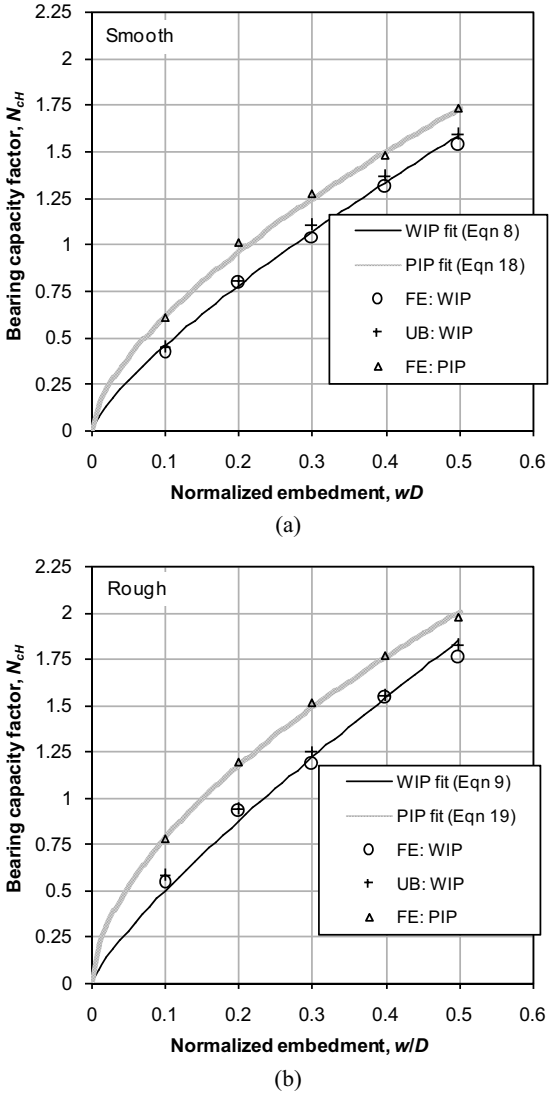

Fig. 6. Bearing capacity factors for horizontal failure

$$N_{cV} = 7.1(\hat{w})^{0.33} \quad \text{(rough PIP pipe)} \tag{18}$$

The heaved soil has a more significant effect on the self-weight factor, N_{swV} (Fig. 5). The agreement between the WIP FE results and the analytical solution based on buoyancy [Eq. (7)] confirms that the bearing capacity and self-weight factors extracted from the finite element (FE) results are consistent. For the PIP case, the self-weight factor is increased by 35% on average. The analytical expression for N_{swV} based on a value of $\lambda = 3$ [Eq. (13)] agrees closely with the data for both the rough and smooth cases.

Horizontal Response, N_{cH} and N_{swH}

The soil heave has a more significant effect on the horizontal bearing capacity factor, N_{cH}, than for the vertical case. An increase in N_{cH} of ~0.25 is evident for $w/D > 0.1$ (Fig. 6). This corresponds to an increase of ~50% at shallow embedments, reducing to ~15% at $w/D = 0.5$. Revision of Eqs. (8) and (9) (WIP case) leads to the following curve fits for the PIP case:

$$N_{cH} = 2.7(\hat{w})^{0.64} \quad \text{(smooth PIP pipe)} \tag{19}$$

$$N_{cH} = 3.0(\hat{w})^{0.58} \quad \text{(rough PIP pipe)} \tag{20}$$

The self-weight factor, N_{swH}, is approximately doubled due to soil heave (Fig. 7). The analytical approximation given by Eq. (13) follows this trend using an idealized heave parameter of $\lambda = 1.6$, which differs from the value fitted to the data for vertical penetration.

Heave Profiles and Pipe-Soil Contact Length

The difference in the back-calculated values of λ for vertical ($\lambda = 3$) and horizontal ($\lambda = 1.6$) movement is linked to the different elevation of the increment of heave caused by each mode of failure. Each value of λ defines the shape of the idealized heave block [Fig. 1(a)] and therefore the mean elevation of the increment of heave, h^*_{heave} [based on Eq. (12*a*)]—a higher value of λ corresponds to a wider idealized heave block and a lower elevation of the next heave increment.

The profiles of heave calculated from the deformed mesh during vertical penetration are shown in Fig. 8 for smooth and rough interfaces and the two extreme values of normalized soil weight, $\gamma' D/s_u$. Also shown are the estimated heave heights, h^*_{heave} [Eq. (12*a*)] for the two selected values of λ. For the smooth case, the

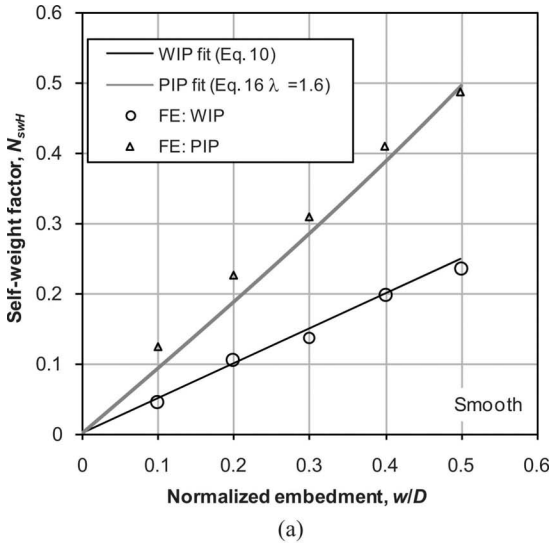

(a)

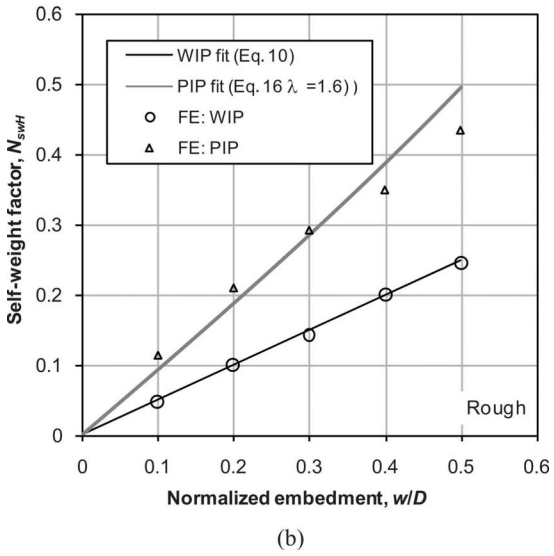

(b)

Fig. 7. Self-weight factors for horizontal failure

heave zone is concentrated closer to the pipe, reflecting a tendency for the penetration mechanism to include shear at the smooth surface of the pipe. Vertical penetration causes a general widening of the heave profile as is evident in Fig. 8. In contrast, horizontal failure involves deformation of the soil close to the pipe surface, which has a higher mean elevation—as is indicated by the lower back-calculated value of λ for N_{cH} compared to N_{cV}. The soil self-weight has a negligible influence on the heave profile for the rough case, but a minor influence is evident for the smooth case.

Fig. 8(e) compares the heave profiles from the FE analysis with the results from a centrifuge model test reported by Dingle et al. (2008). This test used digital image capture and image analysis coupled with close range photogrammetry (White et al. 2003) to monitor the development of heave around a model pipe during penetration into soft kaolin clay. The model represented a 0.8 m diameter pipe penetrating into clay with a shear strength profile of $\sim$2.3 kPa at the surface increasing at a rate of $\sim$3.6 kPa/m. The heave profile shown here—which is the mean of the heave on each side of the pipe—corresponds to an embedment of $w/D=0.35$. At this depth the dimensionless group $\gamma' w/s_u$ is low (0.55), so comparison is made with the weightless FE analyses. The experimental results match the calculated heave profile for the smooth case best. This supports a hypothesis that soft soil is dragged down from the surface by the penetrating pipe resulting in a low pipe-soil interface shear strength relative to the original in situ profile. Moreover, this provides justification for assuming a smooth pipe-soil interface when applying theoretical solutions for evaluation of penetration resistance.

The surface profiles shown in Fig. 8 were used to assess the variation in pipe-soil contact perimeter, p_{contact}, whose magnitude is enhanced by heave. It is important to quantify the pipe-soil contact perimeter since it influences the axial pipe-soil resistance, which is important in the design of pipelines against axial movement during thermal cycles (Bruton et al. 2008).

For the WIP case, the normalized contact perimeter can be calculated from the curved geometry of the pipe as

$$\frac{p_{\text{contact,WIP}}}{D} = \cos^{-1}(1-2\hat{w}) \quad \text{(WIP)} \tag{21}$$

The actual normalized contact perimeter, calculated from the FE analysis, typically exceeds the WIP value by 0.1 (Fig. 9). As the embedment approaches $w/D=0.5$, the WIP and PIP solutions converge, due to the assumption that the soil stands away from the pipe above the midheight.

The expression for h^*_{heave} [Eq. (12*a*)] provides an analytical solution for the contact length for the PIP case

$$\frac{p_{\text{contact,PIP}}}{D} = \cos^{-1}\left(1-2\hat{w}-2\frac{h^*_{\text{heave}}}{D}\right) \quad \text{(PIP)} \tag{22}$$

This expression—using a value of $\lambda=1.6$, which reflects the elevation of the soil close to the pipe—agrees closely with the FE results from this study and the study by Barbosa-Cruz and Randolph (2005), and also the experimental data of Dingle et al. (2008) (Fig. 9). An upper limit of $p_{\text{contact}}/D=\pi/2$ is shown, reflecting the tendency in the FE analysis for the soil to stand free adjacent to the pipe. In practice, soft soil may fall onto the pipe crown, resulting in a further increase in the pipe contact length.

"Local" Embedment

The heave around the pipe can be considered as an increase in the "local" embedment, defined as the elevation of the soil immediately adjacent to the pipe relative to the pipe invert, w_{heave} [Fig. 1(a)]. Embedment depth is an important parameter in the assessment of heat transfer from a pipeline. The rate of heat loss through soil is far slower than through free water, in which convection is the dominant process. When assessing the thermal losses along a pipeline, it is necessary to quantify the proportion of the pipeline which is exposed to free water. In this situation, the relevant embedment depth is the local embedment—which can be approximated as $w_{\text{heave}}=(h^*_{\text{heave}}+w)$ following the terminology of this paper. Similarly, when evaluating the exposure of the pipeline to hydrodynamic loading from waves and currents, it is the local embedment that governs the degree of exposure, not the embedment relative to the original soil surface. However, hydrodynamic action could cause the zones of heave to be eroded, so it may not be appropriate to rely on this local reduction of exposure in the long term.

When considering the force-displacement response of the pipeline, the conventional use of (w/D) should be retained, since all expressions for vertical and horizontal resistance are based on this definition of embedment, even if they include an allowance for heave.

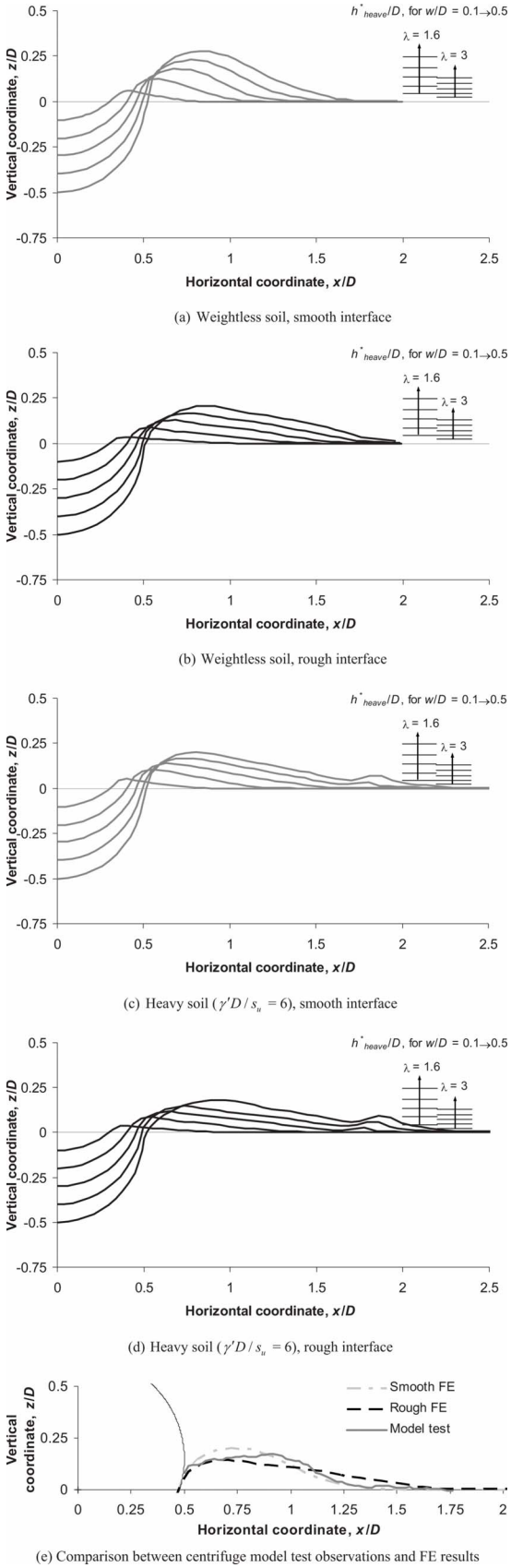

Fig. 8. Profiles of surface heave after vertical penetration

In Fig. 8, the calculated values of h^*_{heave}/D are compared with the profiles of heave generated by the FE analyses. For $\lambda=1.6$, the calculated values of h^*_{heave}/D closely match the local elevation close to the pipe, whereas the values for $\lambda=3$ are more representative of the mean heave elevation. This comparison is in agreement with the back-calculation of $\lambda=1.6$ for N_{swH}—which is governed by local heave—whereas $\lambda=3$ for N_{swV}—which is influenced by the full width of heave.

Fig. 10 compares the "local" and conventional values of embedment for the two back-calculated values of λ. Also shown in Fig. 10 are the "local" embedment values from the FE analyses, based on the highest point of the heave profiles shown in Figs. 8(a–d). These show broad agreement with the idealized local embedment for $\lambda=1.6$, with minor variations depending on soil weight and pipe roughness.

For $\lambda=1.6$, the "local" embedment of the pipe is approximately 50% greater than the embedment relative to the soil surface. At an embedment of $w/D=0.3$, this idealization of the heave indicates contact around the entire lower half of the pipeline, as evident in Fig. 8. This result leads to a consistency between the WIP and PIP results. Figs. 4 and 5 can be used to quantify the reduction in w/D under a given load that arises from considering heave. However, Fig. 10 shows that this reduced embedment relative to the original soil surface is countered by an increased local embedment caused by the heave. These contrasting effects are logical, because the pipe must be surrounded by sufficient soil to provide stability, whether it is WIP or PIP.

Discussion

Example Calculation

The effects of heave are illustrated by considering the calculated response for a typical set of soil and pipe parameters relevant to a deepwater pipeline laid on a soft clay seabed. Based on a diameter of 0.6 m and a specific gravity of 1.2, the pipe weight imposes a nominal bearing pressure of $V/D=6$ kPa. The soil has a unit weight of 6 kN/m^3 and an undrained shear strength of 1.5 kPa.

Fig. 11 shows the calculated embedment and horizontal resistance using these parameters. Three approaches have been used, based on the expressions set out in this paper: (1) WIP, ignoring the self-weight term in the bearing capacity equation, as is common practice; (2) WIP, with inclusion of the self-weight term; and (3) PIP (i.e., including heave), with the self-weight term.

The calculated embedment, w/D, due to the pipe weight is reduced by 35% if the assessment includes the self-weight term and accounts for heave [Fig. 11(a)]. This difference illustrates that the common approach of ignoring the self-weight term is inaccurate. However, the reduced embedment does not lead to an appreciable reduction in the calculated horizontal resistance. Fig. 11(b) shows that the increased value of N_{cH} due to heave, coupled with the inclusion of the self-weight term, means that the PIP approach predicts a horizontal resistance which is comparable to the WIP approach (with or without a self-weight term).

Finally, the calculated values of local embedment, $(h^*_{\text{heave}}+w)/D$—which are more relevant to an assessment of heat loss or hydrodynamic exposure than w/D—are also significantly affected by the inclusion of heave. Comparison of the WIP and PIP cases that include self-weight shows that the PIP approach predicts 15% less embedment (w/D) than the WIP case. However, the local

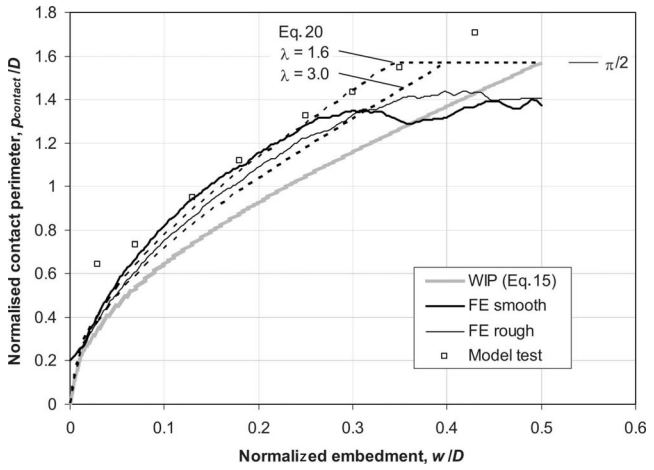

Fig. 9. Pipe-soil contact length during vertical penetration

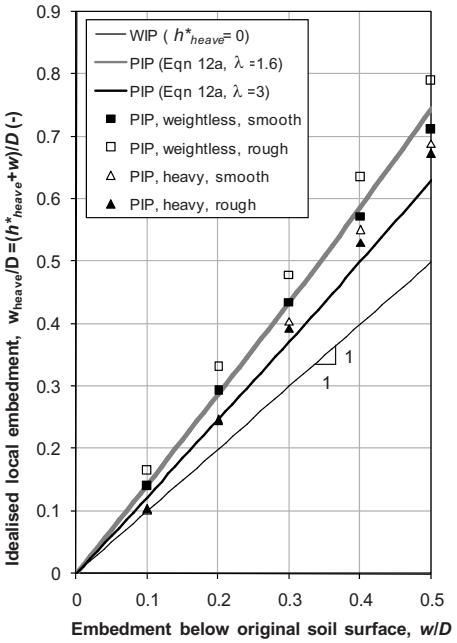

Fig. 10. Idealized local embedment depth

embedment $(h^*_{\text{heave}}+w)/D$ is 25% higher than the WIP value. The inclusion of heave leads to reduced embedment relative to the original soil surface, but enhanced local embedment.

Summary of Solutions

The fitting parameters which have been introduced in this study to capture the variation in vertical and horizontal capacity with pipe embedment are summarized in Table 1 for the various conditions considered. It should be noted that these parameters are only applicable for $w/D \leqslant 0.5$.

The limiting combinations of vertical and horizontal load that can be sustained by a pipeline (or other foundation) can be defined by a yield envelope, in *V-H* load space (Georgiadis and Butterfield 1988; Bransby and Randolph 1998; Merifield et al. 2008). These envelopes can be used to create plasticity models which describe the general response of a pipeline or foundation (Schotman and Stork 1987; Nova and Montrasio 1991; Zhang et al. 2002). The apex points of the yield envelopes are defined by the limiting loads during purely vertical and horizontal movement. Merifield et al. (2008) showed that the yield envelopes for partially embedded WIP pipes are approximately parabolic, with a shape that changes slightly with embedment. If it is assumed that soil self-weight and heave will not change the shape of the envelopes, then the expressions developed in this paper (which correspond to purely vertical or horizontal movement, and therefore the apex points) can be used to calculate the growth of the WIP yield envelopes to account for these effects.

Limitations

To allow generality, the numerical analyses and the resulting calculation methods do not account for all of the processes that govern the embedment and lateral movement of a pipeline in practice. The soil strength is assumed to be uniform, and therefore unaffected by the installation of the pipe, and any subsequent consolidation in the period between embedment and lateral movement. In reality, the installation process may cause a loss of soil strength due to remolding of the soil around the pipe, which will be countered by consolidation under the weight of the pipe (and any contents) prior to lateral movement. The lay process may involve dynamic movement, rather than the static vertical penetration idealized in this analysis.

Also, soil strength typically changes with depth, although the small size of a pipeline means that this variation can often be ignored in practice. However, if necessary, the variation in soil strength with depth can be accounted for by using the soil strength at the pipe invert level. (Aubeny et al. 2005; White and Randolph 2007). This approach is in contrast to the analysis of shallow foundations, for which a representative soil strength is conventionally chosen at a particular depth beneath the founda-

Table 1. Derived Fitting Parameters for Bearing Capacity and Self-Weight Factors

		Vertical			Horizontal		
		$N_{cV}=a\hat{w}^b$			$N_{cH}=c\hat{w}^d$		
Geometry	Interface	a	b	N_{swV}	c	d	N_{swH}
WIP	Smooth	5.66 Eq. (5)	0.32	Eq. (7)	2.72 Eq. (8)	0.78	Eq. (10)
	Rough	7.4 Eq. (6)	0.40		3.26 Eq. (9)	0.82	
PIP	Smooth	5.3 Eq. (15)	0.25	Eq. (13) λ=3	2.7 Eq. (17)	0.64	Eq. (16) λ=1.6
	Rough	7.1 Eq. (16)	0.33		3.0 Eq. (18)	0.58	

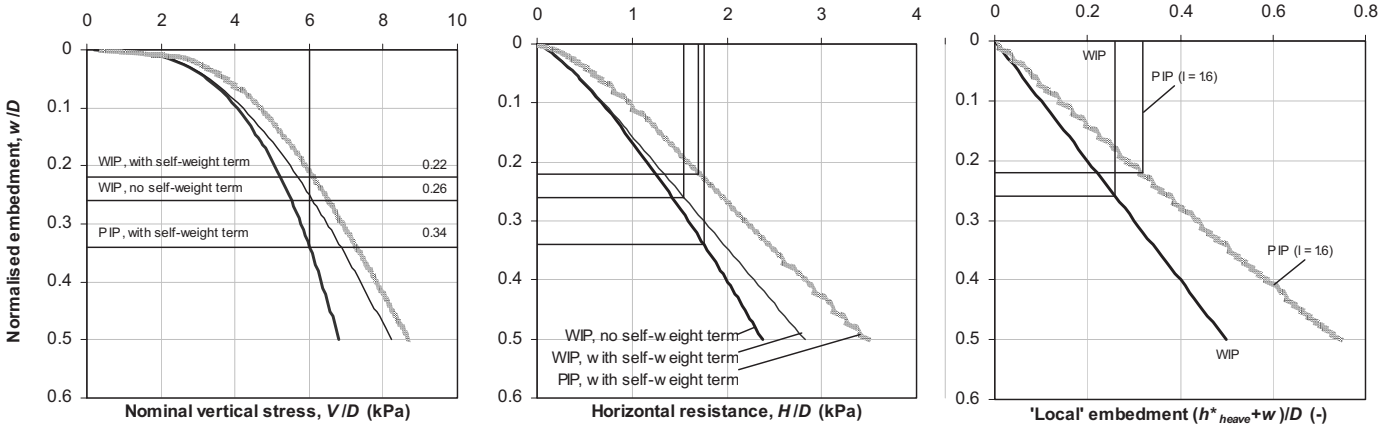

Fig. 11. Example of predicted embedment and horizontal capacity

tion. The pipe invert level is a suitable depth for the case of a pipe because the failure mechanism extends both above and below this level (Merifield et al. 2008; Dingle et al. 2008).

Finally, it is assumed that the pipe does not rotate as it moves laterally, and the lateral movement is conducted at a rate such that no tension can be sustained between the pipe and the soil at the rear. In practice, the rate of lateral movement will affect the possibility of tension being sustained at the rear of the pipe, and also the operative shear strength within the failing soil.

Conclusions

Large deformation finite-element analyses were performed to examine the effect of soil self-weight and heave during pipe penetration; the analyses were supported by a simple analytical approximation of the heave process. This work aims to establish improved methods for predicting the embedment of pipes laid on the seabed.

In soft soil conditions—as are typically found in deep water—an analysis of pipe penetration should include the component of vertical resistance arising from the soil self-weight, since this can be significant. It is shown that the conventional bearing capacity equation—as applied to a flat-based foundation—can be adjusted to correctly reflect the buoyancy arising from the curved shape of a pipe. The contribution of the self-weight surcharge at the pipe invert is quantified by a self-weight factor, N_{swV}, which varies with embedment. This factor is analogous to the conventional bearing capacity factor, N_{cV}, which quantifies the contribution from the soil strength.

For a WIP pipe—i.e., without adjacent heave—the self-weight factor is simply derived from Archimedes' principle of buoyancy. However, the PIP case—i.e., with heave—leads to additional storage of potential energy within the heaved soil, and therefore an increase in the work input required to penetrate the pipe. Using an idealized profile of soil heave, the analytical solution for N_{swV} is extended to the PIP case, for which Archimedes' principle does not apply.

Finite-element analysis was conducted to assess the variation in N_{swV} and N_{cV} with embedment, for both the WIP and PIP cases. The latter case captures the effect of soil heave, and is used to calibrate the analytical approximation of the heave process. A similar calibration procedure is used to generate corresponding factors N_{swH} and N_{cH} for the resistance to horizontal movement.

The FE analyses and experimental observations show that the "local" embedment—due to the raised soil level immediately adjacent to the pipe—significantly exceeds the nominal embedment relative to the original soil surface. This effect partly counteracts the tendency for heave to reduce the nominal embedment by raising the penetration resistance. The heaved soil should not be neglected in design, since this increased local embedment can shield the pipeline from hydrodynamic loading and reduce the rate of heat loss through the surrounding sea water.

The expressions developed for the penetration resistance can be used for routine assessment of static pipe penetration, correctly accounting for the effects of soil self-weight and heave. The analytical approximation to the heave process can be used to assess the likely shielding of the pipe by the raised level of the heaved soil. The solutions for the limiting resistance during vertical and horizontal movement can be used to scale the apex points of previously proposed yield envelopes for general *V-H* loading of partially embedded pipelines, thus allowing the effects of heave and soil self-weight to be incorporated.

Acknowledgments

This work forms part of the activities of the Centre for Offshore Foundation Systems (COFS), established under the Australian Research Council's Research Centres Program and now supported under ARC Grant Nos. FF0561473 and DP0665958, in addition to Centre of Excellence funding from the State Government of Western Australia.

Nomenclature

The following symbols are used in this paper:

A_s = submerged cross-sectional area of foundation;
B^*_{heave} = width of idealized heave block;
D = pipe diameter;
D'_{WIP} = nominal effective diameter;
E = Young's modulus;
f_b = multiplier on Archimedes' fluid buoyancy;
H = horizontal force per unit length of pipe;
h^*_{heave} = height of idealized heave block;
N_c, N_{sw}, N_{cV}, N_{cH}, N_{swV}, N_{swH} = bearing capacity factors;
p_{contact} = length of contact between pipe and soil;

q = bearing stress;
s_u = soil undrained shear strength;
V = vertical force per unit length of pipe;
w = pipe invert embedment below soil surface;
$\hat{w}$ = normalized embedment$=w/D$;
w_{heave} = local embedment;
$\bar{z}$ = mean elevation of displaced soil relative to ground surface;
γ' = submerged unit weight of soil;
δ_w, δ_u = increment of penetration/movement;
λ = berm geometry parameter; and
ν = Poisson's ratio.

References

Aubeny, C. P., Shi, H., and Murff, J. D. (2005). "Collapse loads for a cylinder embedded in trench in cohesive soil." *Int. J. Geomech.*, 5(4), 320–325.

Barbosa-Cruz, E. R., and Randolph, M. F. (2005). "Bearing capacity and large penetration of a cylindrical object at shallow embedment." *Proc., Int. Symp. on Frontiers in Offshore Geotechnics*, Perth, Australia, Taylor and Francis Group, London, 615–621.

Bransby, M. F., and Randolph, M. F. (1998). "Combined loading of skirted foundations." *Geotechnique*, 48(5), 637–655.

Bransby, M. F., and Randolph, M. F. (1999). "The effects of embedment on the undrained response of skirted foundations to combined loading." *Soils Found.*, 39(4), 19–34.

Bruton, D. A. S., White, D. J., Carr, M. C., and Cheuk, C. Y. (2008). "Pipe-soil interaction during lateral buckling and pipeline walking: The SAFEBUCK JIP." *Proc., Offshore Technology Conf.*, Houston, OTC19589.

Cathie, D. N., Jaeck, C., Ballard, J.-C., and Wintgens, J.-F. (2005). "Pipeline geotechnics: State-of-the-art." *Proc., Int. Symp. on Frontiers in Offshore Geotechnics: ISFOG 2005*, Taylor and Francis Group, London, 95–114.

Det Norske Veritas (DNV). (2007). "Recommended practice on-bottom stability design of submarine pipelines." *RP-F109*, Høvik, Norway.

Dingle, H. R. C., White, D. J., and Gaudin, C. (2008). "Mechanisms of pipe embedment and lateral breakout on soft clay." *Can. Geotech. J.*, 45(5), 636–656.

Georgiadis, M., and Butterfield, R. (1988). "Displacements of footings on sand under eccentric and inclined loads." *Can. Geotech. J.*, 25(2), 199–212.

Gourvenec, S. (2008). "Undrained bearing capacity of embedded footings under general loading." *Geotechnique*, 58(3), 177–185.

Hibbit, Karlsson and Sorensen, Inc. (HKS). (2004). *ABAQUS users' manual, Version 6.4*, Providence, R.I.

Martin, C. M., and Randolph, M. F. (2006). "Upper bound analysis of lateral pile capacity in cohesive soil." *Geotechnique*, 56(2), 141–145.

Merifield, R. S., White, D. J., and Randolph, M. F. (2008). "Analysis of the undrained breakout resistance of partially embedded pipelines." *Geotechnique*, 58(6), 461–470.

Murff, J. D., Wagner, D. A., and Randolph, M. F. (1989). "Pipe penetration in cohesive soil." *Geotechnique*, 39(2), 213–229.

Nova, R., and Montrasio, L. (1991). "Settlements of shallow foundations on sand." *Geotechnique*, 41(2), 243–256.

Prandtl, L. (1921). "Eindringungsfestigkeit und festigkeit von schneiden." *Angew. Math. U. Mech.*, 1(1), 15–20.

Randolph, M. F., and White, D. J. (2008). "Upper bound yield envelopes for pipelines at shallow embedment in clay." *Geotechnique*, 58(4), 297–301.

Salgado, R., Lyamin, A. V., Sloan, S. W., and Yu, H. S. (2004). "Two- and three-dimensional bearing capacity of foundations in clay." *Geotechnique*, 54(5), 297–306.

Schotman, G. J. M., and Stork, F. G. (1987). "Pipe-soil interaction: a model for laterally loaded pipelines in clay." *Proc., Offshore Technology Conf.*, Houston, OTC5588.

Skempton, A. W. (1951). "The bearing capacity of clays." *Proc., Building, Research Congress*, Vol. 1, London 180–189.

White, D. J., and Randolph, M. F. (2007). "Seabed characterisation and models for pipeline-soil interaction." *Int. J. Offshore Polar Eng.*, 17(3), 193–204.

White, D. J., Take, W. A., and Bolton, M. D. (2003). "Soil deformation measurement using particle image velocimetry (PIV) and photogrammetry." *Geotechnique*, 53(7), 619–631.

Zhang, J., Stewart, D. P., and Randolph, M. F. (2002). "Modelling of shallowly embedded offshore pipelines in calcareous sand." *J. Geotech. Geoenviron. Eng.*, 128(5), 363–371.